Bioorganic & Medicinal Chemistry Letters 19 (2009) 4634–4638

Contents lists available at ScienceDirect

Bioorganic & Medicinal Chemistry Letters

journal homepage: www.elsevier.com/locate/bmcl

# Discovery of a novel protein kinase B inhibitor by structure-based virtual screening

Jose L. Medina-Franco [a,*], Marc A. Giulianotti [a], Yongping Yu [b], Liangliang Shen [c], Libo Yao [c], Narender Singh [a]

[a] Torrey Pines Institute for Molecular Studies, 11350 SW Village Parkway, Port St. Lucie, FL 34987, USA
[b] College of Pharmaceutical Science, Zhejiang University, Hangzhou 310058, China
[c] Department of Biochemistry and Molecular Biology, The Fourth Military Medical University, Xi'an, Shaanxi 710032, China

ARTICLE INFO

*Article history:*
Received 19 May 2009
Revised 16 June 2009
Accepted 22 June 2009
Available online 25 June 2009

*Keywords:*
AKT
Cancer
Docking
Molecular similarity

ABSTRACT

Protein kinase B (PKB/AKT) is a promising and attractive therapeutic target in anticancer drug development. Herein, we report the findings of virtual screening for novel ATP-competitive inhibitors of AKT-2 using 2D- and 3D-similarity searching and sequential molecular docking with two crystal structures of AKT-2. Our multistep approach led to the identification of a low micromolar AKT-2 inhibitor ($IC_{50}$ = 1.5 μM) with a novel scaffold. The experimentally validated inhibitor represents the starting point for an optimization program.



The serine/threonine kinase B, also known as AKT, has several downstream targets that regulate a number of processes associated with cell growth, differentiation, and division. AKT is frequently amplified and over-expressed in human cancer cells and its inhibition is a promising therapeutic approach for the treatment of cancers.[1,2] There are three known isoforms, AKT-1/PKBα, AKT-2/PKBβ, and AKT-3/PKBγ of AKT. Each one is associated with different types of cancers. AKT-2 is amplified in pancreatic, breast, and ovarian tumors. AKT-3 is over expressed in hormone-insensitive breast and prostate cancers.[1] Aberrations in AKT-1 are less common. AKT has an N-terminal pleckstrin homology (PH) domain, a hinge region, a central kinase domain, and a C-terminal region.[3] The kinase domains have a large homology of more than 85% and the binding pocket residues are the same.[3,4] To date, small molecules targeting the ATP binding site in the kinase domain, and allosteric inhibitors interfering with the PH domain function have been reported.[3–6] AKT inhibitors, either ATP competitors or compounds that interact with regulatory domains, have shown promising activity in cancer treatment. Structural classes of known ATP-competitors include isoquinoline-5-sulfonamides such as **H-89** (Fig. 1),[7] indazole-pyridines, and pyrazole-based compounds (vide infra).

Virtual screening is a powerful approach to identify new drug leads, with several well-documented and successful examples. Many reviews have been recently published that detail these successful cases of compounds that have become approved and are marketed drugs.[8,9] Previous virtual screening studies with the crystal structure of AKT-2 in complex with glycogen synthase kinase-3β peptide (GSK-3β) and 5′-adenylylimidodiphoshate (AMP-PNP)[10] have been described, leading to the identification of three micromolar inhibitors.[11] The fragment-based and iterative structure-based screening methodologies have also resulted in the development of a novel pyrazole-based compound **1** with nanomolar activity (Fig. 1).[12] A crystal structure of AKT-2 in complex with compound **1** has also been reported (PDB code 2UW9).[12] Furthermore, a research group from Abbott has recently described a series of potent and moderately selective indazole-pyridine-based AKT-2 inhibitors. A representative example is **2** in Figure 1 that was obtained after optimizing the activity of a lead compound obtained by high-throughput screening.[13] Despite the promising activity of **2**, both in vitro and in vivo, the molecule showed toxicity along with side effects such as weight loss, malaise, and increased plasma insulin levels.[13] Optimization efforts on compound **2** are on-going.[14] A crystal structure of AKT-2 in complex with **2** has been published (PDB code 2JDR) recently.[15] Overall these two structures, 2UW9 and 2JDR, are quite similar, with backbone root mean square deviation (RMSD) of only 0.36 Å for the whole protein and 0.3 Å for the backbone of binding site residues (residues that are within 5 Å of ligand). A comparison of binding site residues shows that the main contribution to RMSD is due to the flexibility of residues Phe163 and Asp293. In 2JDR, while Asp293 is pointing out, Phe163 extends into the binding cavity and is adjusted parallel to the indoline and pyridine rings of the

* Corresponding author. Tel./fax: +1 772 345 4685.
*E-mail addresses:* jmedina@tpims.org, medinajlmx@yahoo.com.mx (J.L. Medina-Franco).

0960-894X/$ - see front matter © 2009 Elsevier Ltd. All rights reserved.
doi:10.1016/j.bmcl.2009.06.078

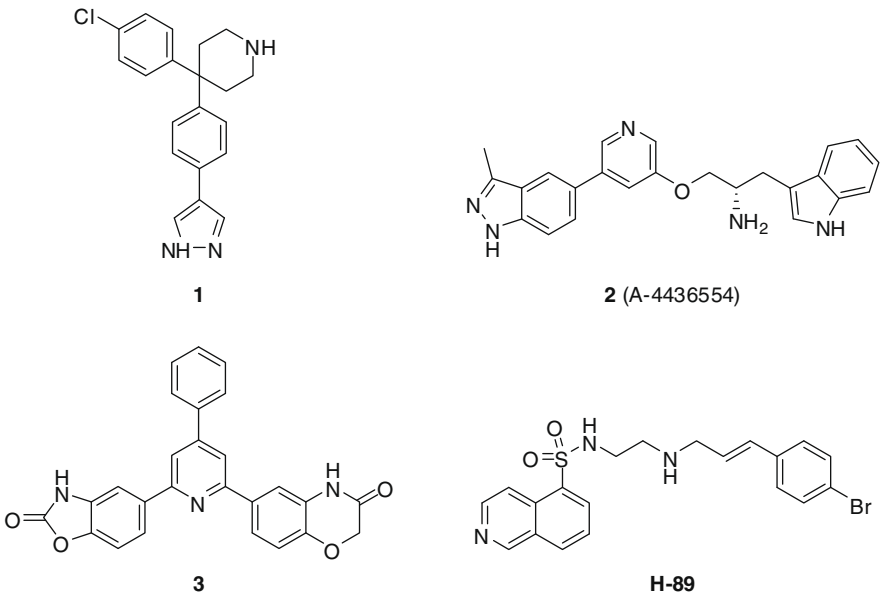


**Figure 1.** Chemical structures of AKT-2 inhibitors. Compound **3** was found in this work.

flexible ligand which has six rotatable bonds. In 2UW9, these two residues are opposite, where Asp263 points inwards, Phe163 is pushed out and has turned ~180° due to the rigid ligand which has only three rotatable bonds. Additionally, the deep binding component of both ligands forms two hydrogen bonds with residues Glu230 and Ala232, and an additional bond with Glu236 in 2UW9 and with Asn280 in 2JDR.

In this work, we have utilized both the ligand and receptor information of these structures described above and performed ligand-based and structure-based virtual screening of a large database of lead-like commercially available compounds to identify novel AKT-2 inhibitors. The virtual screening workflow is depicted in Figure 2.

A subset of 105,937 lead-like compounds implemented in the Molecular Operating Environment (MOE) databases,[16] version 2007, was screened. First, we conducted ligand-based similarity searching using a two-dimensional (2D) and three-dimensional (3D) molecular representations. The chemical structures of **1** and **2** were used as queries (Fig. 2). The 2D-similarities were calculated using the Tanimoto coefficient with MACCS keys (166 bits) as implemented in MOE.[16] The 3D-similarities were obtained using the Rapid Overlay of Chemical Structures (ROCS) software,[17]

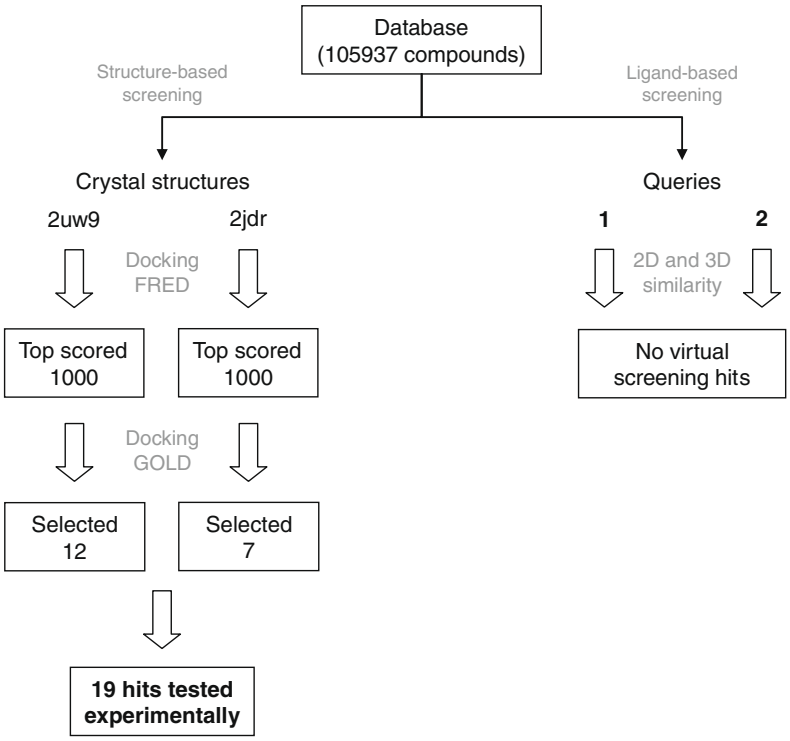


**Figure 2.** Virtual screening workflow.

version 2.3.1, with default parameters. For the screened compound database, a conformer library was generated using the program OMEGA,[18] version 2.2.1 with default parameters. The conformer library has on average 69 conformers per molecule. To compute 3D similarities, the coordinates of **1** and **2** found with the corresponding crystal structures were used as queries. We did not find molecules in the screened database with high 2D and 3D-similarity values to either of the query compounds. The 2D and 3D-similarity profiles to **1** and **2** are summarized in Table S1 in Supplementary data. The highest 2D-similarity observed with any of the queries was 0.87 while the highest 3D-similarity was 0.70 (scaled Combo Score), in both cases to molecule **1**. We also performed similarity searching using the chemical structures of other reported AKT-2 inhibitors as queries, but we again did not find very similar molecules in the screened database (data not shown). Although these results discouraged the selection of compounds for testing based on similarity, the similarity values computed with MACCS keys and ROCS suggested that the topology and shape of the molecules in the compound database was different to what has been reported for AKT-2 inhibitors. Therefore, if structure-based screening identified active molecules (vide infra), we anticipated that such molecules would represent novel chemotypes.

In the second step, we conducted structure-based virtual screening by docking the entire compound database with the above described crystal structures of AKT-2. We performed a two-step docking procedure. First, we docked the entire collection of compounds using a fast docking approach, selected the top ranked molecules and then re-docked the selected compounds with an alternative scoring function (Fig. 2).

For the first, rapid docking, the compound database was docked with the Fast Rigid Exhaustive Docking (FRED) program version 2.2.3.[19] The active site was prepared with Fred-Receptor version 2.2. The corresponding active site box was defined based on the coordinates of the crystallographic ligands and have volumes of 4481 Å$^3$ and 4282 Å$^3$ for 2UW9 and 2JDR, respectively. For both crystal structures, water molecules, peptide substrate (GSK-3β and co-crystal inhibitors were ignored during docking. For the ligands, the same OMEGA-generated conformer library used in 3D-similarity searching (vide supra) was used. The exhaustive search and optimization steps were done with default parameters. For each docked molecule, the top-ranked pose was extracted. For each crystal structure the top 1000 compounds according to Chemgauss3 score were selected (Fig. 2). Selected compounds with FRED were docked using the Genetic Optimization for Ligand Docking (GOLD) program, version 3.2.[20] The Goldscore was used for outcome analysis. The 1000 compounds selected with FRED from docking with 2UW9 were docked with the same crystal structure. The same steps were applied for the molecules selected from docking with 2JDR. For docking with GOLD, the two crystal structures, water molecules, GSK-3β, and co-crystal inhibitors were deleted before docking. The binding site was defined by selecting all atoms within 10 Å of the corresponding crystallographic ligand with the cavity detection mode turned on and using default parameters. A maximum of 10 docking runs per molecule were generated allowing early termination if top three solutions are within 1 Å. Several molecules, docked with the ATP binding site of 2UW9, showed a better Goldscore than the co-crystal inhibitor, **1** (Supplementary data). In contrast, none of the docked molecules with 2JDR showed a better docking score than the co-crystal inhibitor, **2**. Similar observations were made with the docking scores obtained with Chemgauss3. In general, we noticed a low degree of consensus between the top ranked scoring molecules with each crystal structure (2UW9 and 2JDR). In fact, only one molecule was found in common among the top 100 ranked compounds docked with GOLD in both crystal structures.

Finally, a total of 19 compounds were selected from our above described approach and were tested in vitro for AKT-2 inhibition. Out of these 19, 12 compounds were selected from docking with the crystal structure 2UW9 and seven compounds were selected from docking with the crystal structure 2JDR (Fig. 2). The chemical structures of tested compounds are depicted in Figures S1 and S2 in Supplementary data. Overall, the molecules were selected based on one of the two following criteria: a high docking score and/or ability to make hydrogen bonds with Glu230 and Ala232, which is observed in several AKT-2 inhibitors.[12,15,21] Commercial availability at the time of purchase was also considered. One molecule chemically related to the consensus hit among the top scored molecules with GOLD (vide supra) was selected. Selected compounds from docking with the X-ray structure 2UW9 showed a similar or better Goldscore than the score of the co-crystal ligand **1** (vide supra). The top ranked scoring molecule was **3**. Despite the fact that selected molecules from docking with 2JDR had a lower score than the corresponding co-crystal inhibitor **2**, we decided to select molecules for screening searching for putative novel chemotypes (that were different from the selected with 2UW9).

Selected molecules were experimentally evaluated for AKT-2 inhibition with the Z'-LYTE biochemical assay (Invitrogen). The FRET based assay utilizes a ratiometric method for quantifying ATP inhibition. Results are summarized in Table 1. In our studies, compound **3** (Fig. 1), selected from the docking with 2UW9, showed an activity comparable to that of the reference compound **H-89**.[7] All other compounds show no detectable AKT-2 inhibitory activity at 50 μM and 25 μM concentrations. Compound **3** was shown to be a pan-AKT inhibitor with $IC_{50}$ values of 2.6 μM (AKT-1), 1.1 μM (AKT-2), and 4.0 μM (AKT-3).[22] Compound **3** was also screened in a 12 h MTT assay against two different cancer cell lines MDA-MB-468[23] and MDA-MB-453.[24] Against MDA-MB-468, a cell line with PTEN mutations and EGFR amplification to which an AKT-P inhibitor should have a modest response, compound **3** had an $EC_{50}$ of 3.8 μM. While against MDA-MB-453, a cell line with HER2 amplification and PIK3CA mutations that should be very sensitive to AKT phosphorylation inhibition, it had an $EC_{50}$ of 10.0 μM.

Notably, the active compound **3** showed the best Golscore in docking with 2UW9 (vide supra). In order to describe the ligand-binding site interactions, the binding mode found by Goldscore within the binding geometry of **2** (PDB 2UW9) was subject to full energy minimization using the MMFF94x force field implemented in MOE until the gradient 0.001 was reached. The default parameters implemented into the MOE's LigX application were used. Figure 3A depicts the optimized binding model of **3** with AKT-2. The corresponding 2D interaction map is depicted in Figure 3C. According to the binding model, **3** makes hydrogen bonds with the side chain atoms of Thr213, Thr292, and Asp293. A π–π interaction was also predicted between the phenyl ring of **3** and Phe443 (Fig. 3B). We further investigated the binding mode of our tested compound with the AUTODOCK4 program.[25,26] The program predicted a very similar binding mode, and also suggested an alternative binding mode where the molecule is flipped by 180° along the phenyl ring, while keeping the same deep binding pocket interactions. A comparison with the predicted binding mode for **H-89** is also shown as a 3D model and 2D interaction map in Figure 3B

**Table 1**
Inhibitory activity of **3** with three AKT isoforms ($IC_{50}$ values in μM)

| Compound | AKT-1 | AKT-2 | AKT-3 |
|---|---|---|---|
| **3** | 2.6 | 1.5 | 4.0 |
| **H-89**[a] | 1.6 | 0.3 | 0.2 |

[a] Values are historical values reported by Caliper with the same assay condition used to calculate the $IC_{50}$ for compound **3**.

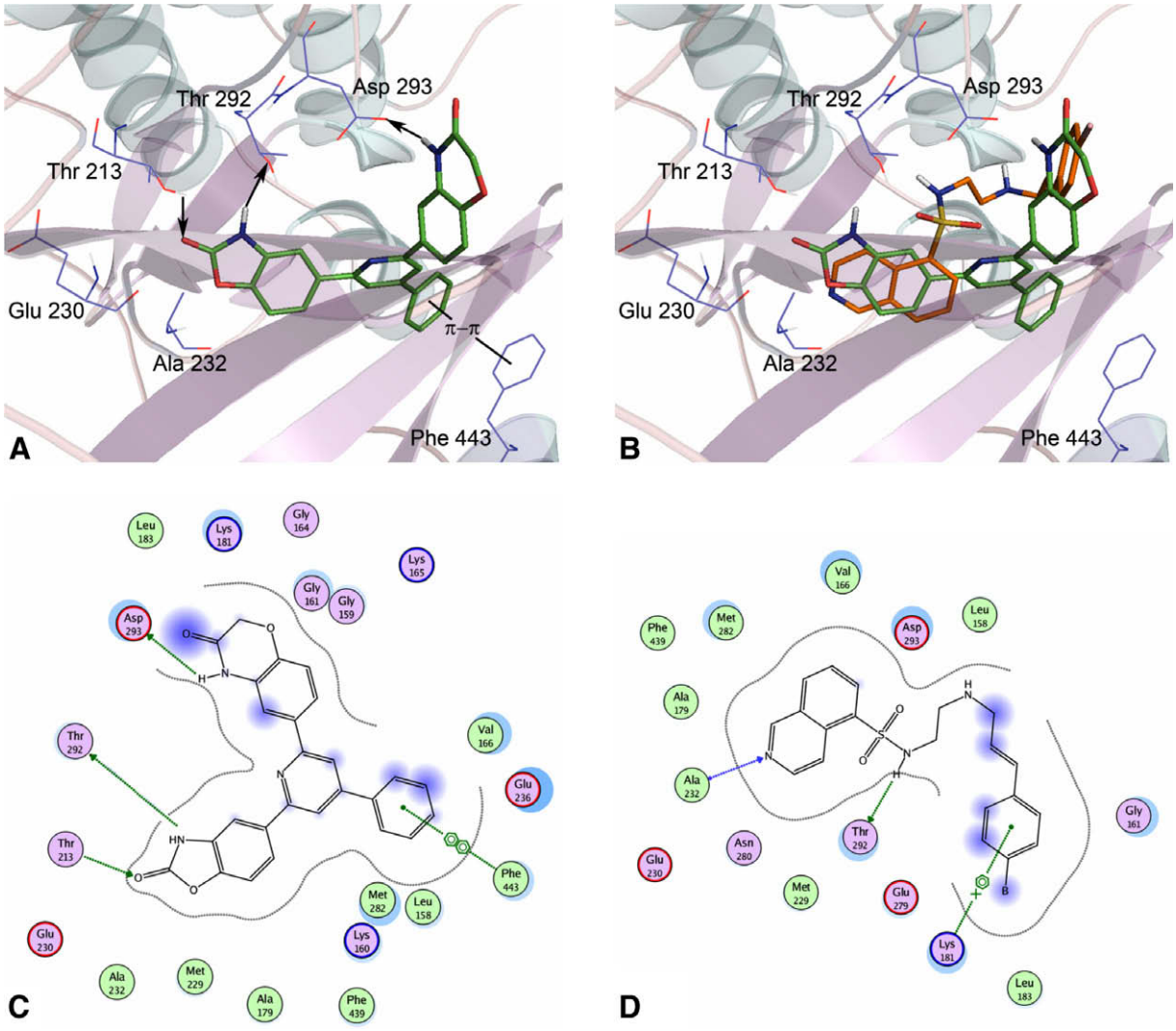


**Figure 3.** Optimized docking model of **3** and **H-89** with AKT-2. (A) 3D models showing docked **3**; (B) 3D model showing superimposed docked **3** and **H-89**. Hydrogen bonds are depicted with arrows. Non-polar hydrogen atoms are omitted for clarity. (C) and (D) showing 2D interaction diagrams of **3** and **H-89**, respectively. Amino acid residues within 4.5 Å of docked compounds are shown. The active site residues are represented as follows: polar residues in pink, hydrophobic residues in green, acidic residues with a red contour ring, basic residues with a blue contour ring. Green arrows indicate hydrogen bonding to side chain atoms, respectively. Blue 'clouds' on ligand atoms indicate the solvent exposed surface area of ligand atoms (darker and larger clouds means more solvent exposure). Light-blue 'halos' around residues indicate the degree of interaction with ligand atoms (larger, darker halos means more interaction). The dotted contour reflects steric room for methyl substitution. The contour line is broken if it is close to an atom which is fully exposed.

and D, respectively. Overall the docked pose of **H-89** was oriented in a similar fashion as compound **3**. The major differences were in the hydrogen bond interactions of binding site residues. The hydrogen bonds shown by binding site residues Thr213 and Asp293 in compound **3** were not observed with docked **H-89** (Fig. 3D). Instead Ala232 and Lys181 were two binding site residues that hydrogen bonded with **H-89**. The hydrogen bond with Thr292 was observed in both, compound **3** and **H-89** (Fig. 3).

Despite the fact that **3** showed no selectivity for AKT-2, this molecule has a novel chemotype with AKT activity. The very similar ATP binding sites of AKT-1 and AKT-2[3,4] represent a significant challenge in the virtual screening for specific inhibitors. However, **3** with its novel scaffold is a promising starting point to search in a different area of chemical space[27] for selective and potent inhibitors. A first step toward the exploration of new areas of chemical space would be using **3** as a query in similarity searching.

In conclusion, a novel low micromolar AKT-2 inhibitor was identified by multistep virtual screening. The molecule has a different scaffold with respect to published AKT-2 inhibitors and represents the starting point for an optimization program. Further development of **3** will include exploring the SAR required to obtain desired AKT selectivity.

## Acknowledgments

The authors are grateful to Dr. Colette Dooley for the valuable comments. The authors also wish to thank Kyle Kryak for his assistance. This work was supported by the State of Florida, Executive Office of the Governor's Office of Tourism, Trade, and Economic Development. Yongping Yu thanks the National Nature Science Foundation of China (30772652). The authors thank OpenEye Scientific Software, Inc., for providing FRED, Fred-Receptor, OMEGA and ROCS programs.

## Supplementary data

2D and 3D-similarity profile of the compound database with **1** and **2** (Table S1). Chemical structures of 19 selected compounds from virtual screening (Figs. S1 and S2). Supplementary data

associated with this article can be found, in the online version, at doi:10.1016/j.bmcl.2009.06.078.

## References and notes


1. Hennessy, B. T.; Smith, D. L.; Ram, P. T.; Lu, Y. L.; Mills, G. B. *Nat. Rev. Drug Disc.* **2005**, *4*, 988.
2. Cheng, J. Q.; Lindsley, C. W.; Cheng, G. Z.; Yang, H.; Nicosia, S. V. *Oncogene* **2005**, *24*, 7482.
3. Cheng, G. Z.; Park, S.; Shu, S. K.; He, L. L.; Kong, W.; Zhang, W. Z.; Yuan, Z. Q.; Wang, L. H.; Cheng, J. Q. *Curr. Cancer Drug Targets* **2008**, *8*, 2.
4. Lindsley, C. W.; Barnett, S. F.; Layton, M. E.; Bilodeau, M. T. *Curr. Cancer Drug Targets* **2008**, *8*, 7.
5. Kumar, C. C.; Madison, V. *Oncogene* **2005**, *24*, 7493.
6. Mahadevan, D.; Powis, G.; Mash, E. A.; George, B.; Gokhale, V. M.; Zhang, S. X.; Shakalya, K.; Du-Cuny, L.; Berggren, M.; Ali, M. A.; Jana, U.; Ihle, N.; Moses, S.; Franklin, C.; Narayan, S.; Shirahatti, N.; Meuillet, E. J. *Mol. Cancer Ther.* **2008**, *7*, 2621.
7. Reuveni, H.; Livnah, N.; Geiger, T.; Kleid, S.; Ohne, O.; Cohen, I.; Benhar, M.; Gellerman, G.; Levitzki, A. *Biochemistry* **2002**, *41*, 10304.
8. Muegge, I. *Mini-Rev. Med. Chem.* **2008**, *8*, 927.
9. Guido, R. V. C.; Oliva, G.; Andricopulo, A. D. *Curr. Med. Chem.* **2008**, *15*, 37.
10. Yang, J.; Cron, P.; Good, V. M.; Thompson, V.; Hemmings, B. A.; Barford, D. *Nat. Struct. Biol.* **2002**, *9*, 940.
11. Forino, M.; Jung, D.; Easton, J. B.; Houghton, P. J.; Pellecchia, M. *J. Med. Chem.* **2005**, *48*, 2278.
12. Saxty, G.; Woodhead, S. J.; Berdini, V.; Davies, T. G.; Verdonk, M. L.; Wyatt, P. G.; Boyle, R. G.; Barford, D.; Downham, R.; Garrett, M. D.; Carr, R. A. *J. Med. Chem.* **2007**, *50*, 2293.
13. Luo, Y.; Shoemaker, A. R.; Liu, X. S.; Woods, K. W.; Thomas, S. A.; de Jong, R.; Han, E. K.; Li, T. M.; Stoll, V. S.; Powlas, J. A.; Oleksijew, A.; Mitten, M. J.; Shi, Y.; Guan, R.; McGonigal, T. P.; Klinghofer, V.; Johnson, E. F.; Leverson, J. D.; Bouska, J. J.; Mamo, M.; Smith, R. A.; Gramling-Evans, E. E.; Zinker, B. A.; Mika, A. K.; Nguyen, P. T.; Oltersdorf, T.; Rosenberg, S. H.; Li, Q.; Giranda, V. L. *Mol. Cancer Ther.* **2005**, *4*, 977.
14. Zhu, G. D.; Gandhi, V. B.; Gong, J. C.; Thomas, S.; Woods, K. W.; Song, X. H.; Li, T. M.; Diebold, R. B.; Luo, Y.; Liu, X. S.; Guan, R.; Klinghofer, V.; Johnson, E. F.; Bouska, J.; Olson, A.; Marsh, K. C.; Stoll, V. S.; Mamo, M.; Polakowski, J.; Campbell, T. J.; Martin, R. L.; Gintant, G. A.; Penning, T. D.; Li, Q.; Rosenberg, S. H.; Giranda, V. L. *J. Med. Chem.* **2007**, *50*, 2990.
15. Davies, T. G.; Verdonk, M. L.; Graham, B.; Saalau-Bethell, S.; Hamlett, C. C. F.; McHardy, T.; Collins, I.; Garrett, M. D.; Workman, P.; Woodhead, S. J.; Jhoti, H.; Barford, D. *J. Mol. Biol.* **2007**, *367*, 882.
16. Molecular Operating Environment (MOE), version 2007; Chemical Computing Group: Montreal, Quebec, Canada. Available at http://www.chemcomp.com (accessed May 2009).
17. Rapid Overlay of Chemical Structures (ROCS), version 2.3.1; OpenEye Scientific Software: Santa Fe, NM. Available at http://www.eyesopen.com (accessed May 2009).
18. OMEGA, version 2.2.1; OpenEye Scientific Software Inc.: Santa Fe, NM. Available at http://www.eyesopen.com (accessed May 2009).
19. McGann, M. R.; Almond, H. R.; Nicholls, A.; Grant, J. A.; Brown, F. K. *Biopolymers* **2003**, *68*, 76.
20. Jones, G.; Willett, P.; Glen, R. C.; Leach, A. R.; Taylor, R. *J. Mol. Biol.* **1997**, *267*, 727.
21. Heerding, D. A.; Rhodes, N.; Leber, J. D.; Clark, T. J.; Keenan, R. M.; Lafrance, L. V.; Li, M.; Safonov, I. G.; Takata, D. T.; Venslavsky, J. W.; Yamashita, D. S.; Choudhry, A. E.; Copeland, R. A.; Lai, Z. H.; Schaber, M. D.; Tummino, P. J.; Strum, S. L.; Wood, E. R.; Duckett, D. R.; Eberwein, D.; Knick, V. B.; Lansing, T. J.; McConnell, R. T.; Zhang, S. Y.; Minthorn, E. A.; Concha, N. O.; Warren, G. L.; Kumar, R. *J. Med. Chem.* **2008**, *51*, 5663.
22. Caliper LifeSciences. Available at http://www.caliperls.com/products/akt2-pkbb-h.htm (accessed May 2009).
23. Lu, Y. L.; Lin, Y. Z.; LaPushin, R.; Cuevas, B.; Fang, X. J.; Yu, S. X.; Davies, M. A.; Khan, H.; Furui, T.; Mao, M. L.; Zinner, R.; Hung, M. C.; Steck, P.; Siminovitch, K.; Mills, G. B. *Oncogene* **1999**, *18*, 7034.
24. She, Q.-B.; Chandarlapaty, S.; Ye, Q.; Lobo, J.; Haskell, K. M.; Leander, K. R.; DeFeo-Jones, D.; Huber, H. E.; Rosen, N. *PLoS ONE* **2008**, *3*, e3065.
25. Huey, R.; Morris, G. M.; Olson, A. J.; Goodsell, D. S. *J. Comput. Chem.* **2007**, *28*, 1145.
26. Morris, G. M.; Huey, R.; Lindstrom, W.; Sanner, M. F.; Belew, R. K.; Goodsell, D. S.; Olson, A. J. *J. Comput. Chem.* **2009**, in press, doi:10.1002/jcc.21256.
27. Medina-Franco, J. L.; Martinez-Mayorga, K.; Giulianotti, M. A.; Houghten, R. A.; Pinilla, C. *Curr. Comput. Aided Drug Des.* **2008**, *4*, 323.